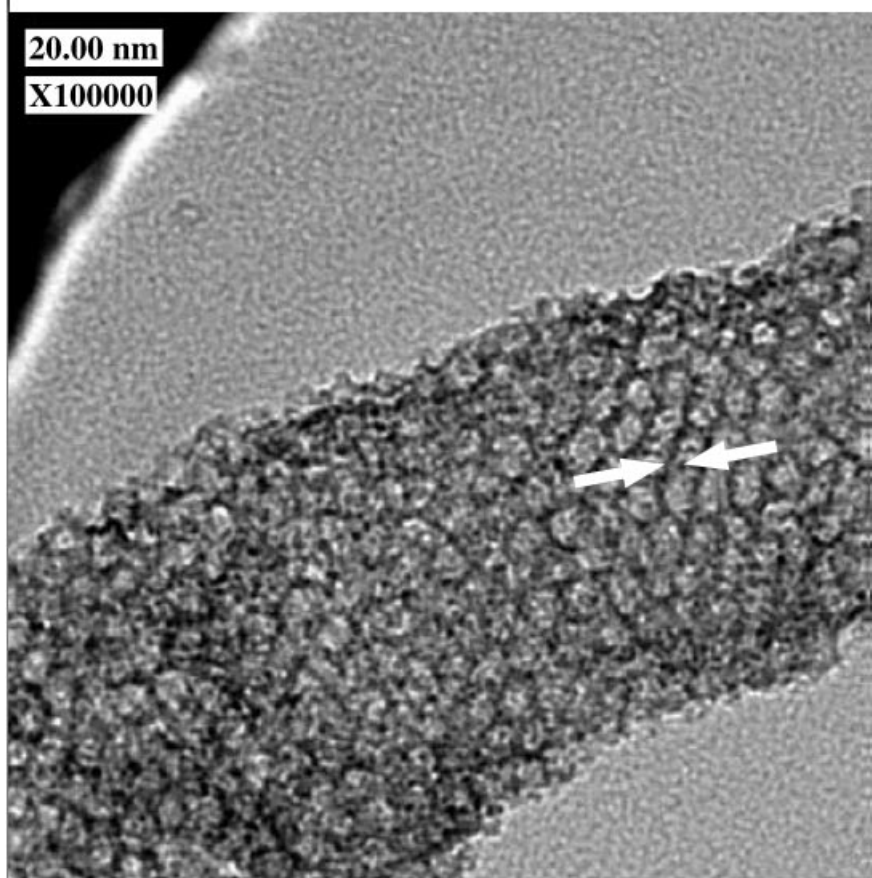
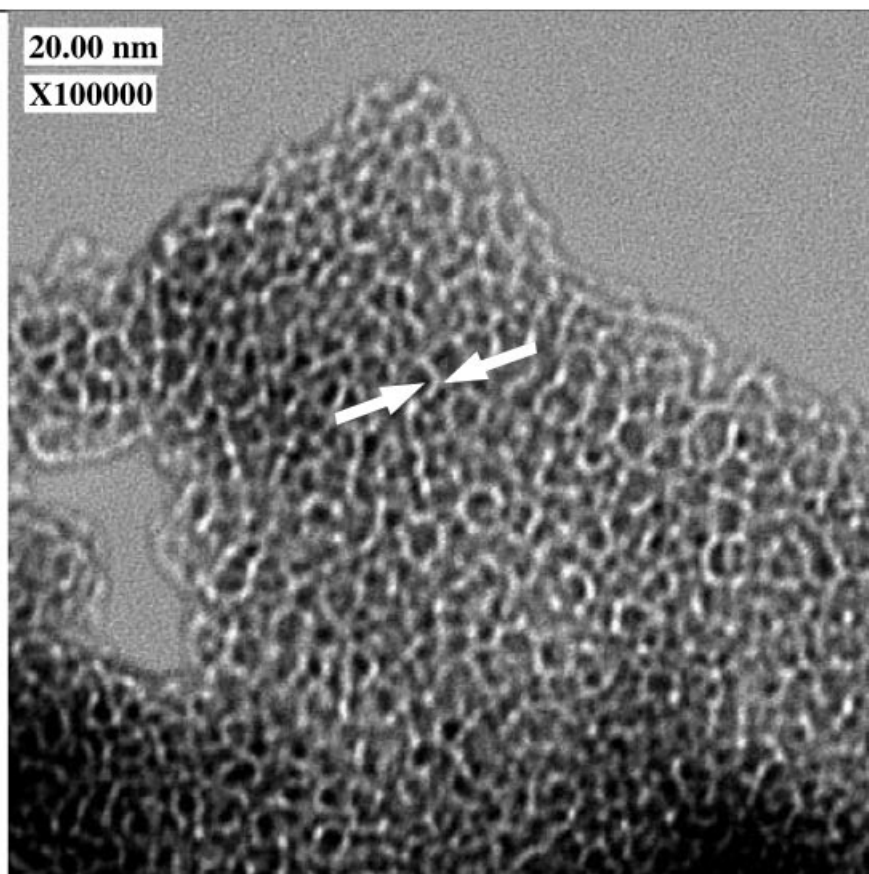


HR-TEM micrographs of an Al-MCM-41 support (right) and an MoO<sub>x</sub>/Al-MCM-41 composite (45 wt% MoO<sub>3</sub>; shown below) prepared by an ultrasonically controlled reaction.



The wall thickness, indicated by the arrows, changes from 1.5 nm (above) to 2.3 nm (left) upon the deposition of the MoO<sub>3</sub> in the mesopores.

## Using Sonochemical Methods for the Preparation of Mesoporous Materials and for the Deposition of Catalysts into the Mesopores

Aharon Gedanken,<sup>\*,[a]</sup> Xianghai Tang,<sup>[a]</sup> Yanquin Wang,<sup>[a]</sup> Nina Perkas,<sup>[a]</sup> Yuri Koltypin,<sup>[a]</sup> Miron V. Landau,<sup>[b]</sup> Leonid Vradman,<sup>[b]</sup> and Mordechay Herskowitz<sup>[b]</sup>

**Abstract:** Ultrasound radiation can be used to synthesize a variety of mesoporous materials. The reaction time is considerably shorter than the conventional methods. Ultrasonic waves can be further used for the insertion of amorphous nanosized catalysts into the mesopores. A detailed study demonstrates that the nanoparticles are deposited as a monolayer on the inner mesopores walls without blocking them. When the ultrasonically prepared catalyst/mesoporous-substrate composite is used in catalysis a high conversion into product is obtained.

**Keywords:** interfaces • mesoporous materials • nanostructures • scanning probe microscopy • sonochemistry

### Introduction

In a recent review article the synthesis of mesoporous silica is considered as one of the four most important discoveries in solid-state and materials science in the last decade.<sup>[1]</sup> Indeed ever since the first report of its synthesis in 1992,<sup>[2, 3]</sup> mesoporous silica and other mesoporous materials have attracted much attention. This is reflected in close to 2000 or more papers in the literature. The interest in these compounds is due to their importance in the many applications in catalytic and separation technologies. Several reviews have already been written on these materials.<sup>[4-6]</sup>

The original sol–gel synthesis was conducted at 100 °C, and used C<sub>16</sub>H<sub>33</sub>(CH<sub>3</sub>)<sub>3</sub>NOH/Cl as the surfactant. The surfactant

was added to an acidic solution of sodium silicate and the mixture was heated for 144 hours. Decreasing the heating temperature and shortening the reaction time has been achieved in the synthesis of MCM-41;<sup>[7]</sup> however, the silica groups of the material were poorly condensed, and the product was less thermally stable than those synthesized at higher temperatures. This report will not review the enormous amount of synthetic routes varying parameters such as the surfactants, structural components, temperatures, and others that have been experimented over the last eight years. It will concentrate only on a new method that have been developed lately for the synthesis of mesoporous materials, that is, the sonochemical method. Sonochemistry has been used not only for the preparation of the mesoporous materials, but also for the insertion of amorphous nanoparticles into the mesopores. Suslick has demonstrated that these amorphous nanoparticles are catalytically more active than their corresponding nanocrystalline compounds.<sup>[8]</sup>

Sonochemistry arises from the acoustic cavitation phenomenon, that is, the formation, growth, and implosive collapse of bubbles in a liquid medium.<sup>[8]</sup> The extremely high temperatures (> 5000 K), pressure (> 20 Mpa), and very high cooling rates (> 10<sup>10</sup> K s<sup>-1</sup>)<sup>[9]</sup> attained during cavitation collapse lead to many unique properties in the irradiated solution. For example, the sonication of a volatile precursor in a nonvolatile solvent would yield amorphous nanoparticles. This is due to the high cooling rates that prevent the crystallization of the sonication products.

We have recently demonstrated that ultrasound radiation can also be used for the preparation of mesoporous materials. Mesoporous silica, MCM-41,<sup>[10]</sup> titania,<sup>[11]</sup> and YSZ (yttria stabilized zirconia)<sup>[12]</sup> were all prepared by this method. In addition, straight-extended layered mesostructures based on transition metal (Fe, Cr) and rare earth (Y, Ce, La, Sm, Er) oxides were also synthesized sonochemically.<sup>[13]</sup> The main advantage of the sonication method is in the short irradiation time. In most cases the reaction time was three hours. The longest sonication period was six hours. It was applied for the synthesis of mesoporous YSZ and caused the transformation of the product from a layered to hexagonal mesostructure due to this prolonged irradiation time. The thermal stability of the

[a] Prof. A. Gedanken, Dr. X. Tang, Dr. Y. Wang, Dr. N. Perkas, Dr. Yu. Koltypin  
Department of Chemistry, Bar-Ilan University  
Ramat-Gan, 52900 (Israel)  
Fax: (+972)-3-535-1250  
E-mail: gedanken@mail.biu.ac.il

[b] Prof. M. V. Landau, L. Vradman, Prof. M. Herskowitz  
Blechner Center for Industrial Catalysis and  
Process Development, Chemical Engineering Department  
Ben-Gurion University of the Negev  
Beer-Sheva 84105 (Israel)

product is another advantage of the technique. We were able to show that the MCM-41 obtained sonochemically is more stable than MCM-41 prepared by conventional hydrothermal methods.<sup>[14]</sup> This was demonstrated when our product was treated with pure water, its crystallinity changed only a little after heating under reflux for six hours, and decreased by approximately 65% after heating under refluxing for twelve hours. In the literature<sup>[14]</sup> the MCM-41 prepared by using conventional hydrothermal methods became amorphous after refluxing for twelve hours.

### Synthetic Methods

Since the reaction conditions for the preparation of mesoporous silica and titania have already been reported the synthesis of YSZ will exemplify the typical sonication conditions. The molar ratio of Y/Zr was 1:1, and the molar ratio of (Y + Zr)/SDS/urea was 1:2:30 (SDS = sodium dodecyl sulfate). Typically, Y<sub>2</sub>O<sub>3</sub> (0.28 g) was dissolved in a minimum amount of HNO<sub>3</sub> and heated until it dried. Distilled water (60 mL) was then added to this mixture. ZrO(NO<sub>3</sub>)<sub>2</sub> (0.57 g), SDS (2.88 g), and urea (9.0 g) were added then added to this solution under stirring. The pH of this mixture was approximately 4.5. The mixture was sonicated at room temperature for 1.5, 3, or 6 hours by a high-intensity ultrasonic probe (Misonix, XL sonifier, 1.13 cm diameter Ti horn, 20 KHz, 100 Wcm<sup>-2</sup>). During sonication, the temperature of the reaction mixture rose to approximately 80 °C. After sonication, the suspension was centrifuged, washed with deionized water and ethanol, and dried in vacuum. For the removal of the surfactant, sodium acetate was used, following Yada's method.<sup>[15]</sup> In addition to using SDS as the surfactant for the preparation of mesoporous YSZ, we have also successfully employed carboxylic acids as the templating agents for its synthesis. The as-prepared materials maintain their original hexagonal structure after calcination at 400 °C for one hour. Unlike the SDS synthesis which used zirconyl nitrate as the Zr source, Zr(*i*OPr)<sub>4</sub> was employed in the latter reaction. Layered and hexagonal mesostructures were obtained as the products after sonication of 1.5 hours, when SDS was used as the surfactant. A longer irradiation time of six hours caused a lamellar to hexagonal transition. When carboxylic acids were used as the templating agents, only a wormhole mesophase was detected. The original wormhole structure remained intact even after calcination at 400 °C for one hour.

Straight-extended layered mesostructures based on transition metal (Fe, Cr) and rare earth (Y, Ce, La, Sm, Er) oxides were synthesized by sonication for three hours. In this synthesis, sodium dodecyl sulfate (SDS) was used as the surfactant template, urea was used as the precipitating agent, and the nitrate salts of metals were used as the precursors of metal ions. Long-range straight-extended layered structures are obtained for all as-prepared samples, except for Cr-, and Er-based layered structures, for which short-range layered structures are obtained. These straight-extended layered structures are consistent with most layered mesostructured solids, such as the silica/surfactant<sup>[16]</sup> and zirconia/surfactant<sup>[17]</sup> systems, but very different from that prepared under heat-

ing.<sup>[15, 18]</sup> In all the sonication processes in which SDS was used as the templating agent, the interlayer spacings from TEM are in the range of 3.3–4.8 nm. This spacing can be explained by assuming that SDS molecules are arranged as a bilayer between the inorganic layers.

### Advantages and Mechanism of the Sonochemical Method

The main advantage in the application of ultrasound radiation to the synthesis of the various mesoporous materials is the drastic reduction in the fabrication time from days<sup>[3]</sup> to 3–6 hours. In addition in the case of MCM-41 we have demonstrated that the walls of the sonochemical product were thicker than those obtained conventionally (see Table 1 ref. [11]). We have already mentioned above the thermal stability resulting from these thicker walls. During the

Table 1. Physicochemical properties of iron oxide catalyst prepared by the sonication method.

Support	Fe <sub>2</sub> O <sub>3</sub> [mass %]		E <sub>b</sub> [eV] <sup>[a]</sup>		Conversion of cyclohexane [%]
	EDX	AAS	Fe <sub>2P3/2</sub>	Ti <sub>2P3/2</sub>	
Fe <sub>2</sub> O <sub>3</sub>	100	100	710.5	–	16.5
Fe <sub>2</sub> O <sub>3</sub> /TiO <sub>2</sub> (Degussa P-25)	20.3	12.0	710.6	457.6	21.3
Fe <sub>2</sub> O <sub>3</sub> /TiO <sub>2</sub> (MSPT)	18.7	14.5	710.9	458.7	25.8

formation of the framework, despite the agitation of the ultrasound which helps to disperse the small silica oligomers more homogeneously in the mixture, the formation of hot spots within the surfactant-silicate interface may accelerate the silica polymerization, which is slow and rate-limiting under normal conditions. Thus the fabrication of the mesostructure can be achieved more efficiently. On the one hand, acoustic cavitation etches the surfactant–silicate micelles on the surface; this results in a coarse outer surface or even the fragmentation of the micelles. On the other hand, hot spots accelerate the condensation of surface silanol groups among micelles; in this way ultrasound radiation accelerates the formation of MCM-41 framework and the growth of particles. This twofold function of ultrasound radiation results in the particles of sonochemical product being bigger and more aggregated than those prepared conventionally, though the latter are more uniform in size. It is also worth noting that ultrasound radiation did not destroy the micellar structure.<sup>[19]</sup>

### Inserting Nanocatalysts Sonochemically into Mesopores

The discovery of mesoporous materials has led immediately to the development of many experimental methods for the deposition of materials, especially catalysts, into the mesopores. In many cases a precursor for the catalyst was mixed with the precursor for the mesoporous material and in one

step the catalyst is incorporated in the skeleton of the mesoporous structure.<sup>[20]</sup> In other cases materials have been introduced into the prepared pores by impregnation,<sup>[21]</sup> chemical vapor deposition,<sup>[22]</sup> deposition–precipitation method,<sup>[23]</sup> or electrochemical methods.<sup>[24]</sup>

We have deposited Mo oxide, and Co–Mo oxides into MCM-41 as well as into the pores of Al-MCM-41. We have also anchored Fe<sub>2</sub>O<sub>3</sub> into the mesopores of titania. In addition to the characterization studies of the composite catalyst–mesoporous product, catalytic studies have also been conducted.

The typical sonochemical reaction is performed as follows: a slurry of Al-MCM-41 in decalin (120 mL) containing dissolved Mo(CO)<sub>6</sub> and/or Co(CO)<sub>3</sub>NO. The sonication was carried out by employing a high-intensity Ti-horn (20 kHz, 100 W cm<sup>-2</sup>) sonicator under ambient air at room temperature for periods of up to four hours. The solid product was separated by centrifugation, thoroughly washed with dry pentane, and dried in vacuum at room temperature. In all cases we have based the sonochemical synthesis on reactions that have been developed in our laboratory.<sup>[25, 26]</sup> Characterization measurements have demonstrated that nanosized amorphous catalysts were anchored in the pores.

IR measurements were always the first to be performed. In all cases no peaks in the region of 2000 cm<sup>-1</sup> of the C–O stretching vibrational mode were detected for the products of the insertion of Fe(CO)<sub>5</sub>, or Mo(CO)<sub>6</sub> and/or Co(CO)<sub>3</sub>NO into the mesoporous support. This is an indication that the precursor is not being deposited on the walls of the support, but rather the sonication product. The wide-angle X-ray diffraction (XRD) pattern of the deposition products did not show distinct peaks, as a result of the amorphous nature of the sonication products.

For the sake of brevity we will demonstrate the methodology undertaken for the examination of the sonochemical deposition only for Mo oxide deposited in the pores of Al-MCM-41. The chemical reaction leading to the formation of the Mo oxide has been previously reported [Eq. (1)].<sup>[26, 27]</sup>



The chemical composition of solid catalysts (wt %, average of five measurements at different points of the solid) was measured by SEM-EDAX (scanning electron microscopy/energy-dispersive X-ray analysis) method. The sonication yield of Mo(CO)<sub>6</sub> in decalin solution (with a starting concentration of 4.75 g of Mo(CO)<sub>6</sub>/L), as reflected in the amount of deposited Mo oxide phase (calculated as MoO<sub>3</sub> from EDAX data) was probed. The yield of the Mo oxide in presence of Al-MCM-41 support was greater than in the absence of Al-MCM-41 support (Figure 1a). It implies that the number of

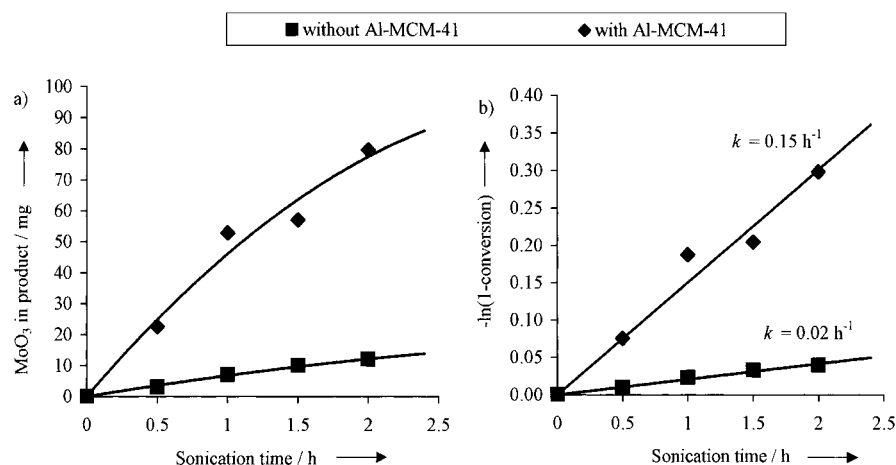


Figure 1. a) The amount of MoO<sub>3</sub> and b) the kinetics of its formation as a function of sonication time in the presence and absence of Al-MCM-41.

collapsing bubbles is enhanced due to the presence of the solid surfaces of the mesoporous material.

The significant increase of Mo oxide deposition rate after its insertion into the Al-MCM-41 support indicates not only that there are more collapsing bubbles, but also that there is a strong interaction between the support and Mo oxide. This interaction is induced by sonication, since attempts to deposit Mo or Co oxides onto Al-MCM-41 by the same procedure without sonication were unsuccessful. The ultrasonically induced chemical interaction between the Mo precursor (carbonyl or oxide) and Al-MCM-41-support should yield new silicate-type compounds with characteristic chemical state of Mo, Si, and O atoms. This was demonstrated from the binding energies of characteristic electrons measured by X-ray photoelectron spectroscopy (XPS) for pure Al-MCM-41, Mo oxide deposited under sonication in the absence of Al-MCM-41, and for MoO<sub>x</sub>-Al-MCM-41 composites obtained sonochemically. The XPS spectra of Si 2p, O 1s, and Mo 3d electrons of those samples are shown in Figure 2. It is clear that the Mo deposition created a new band in spectrum of the Si 2p electrons at binding energy of 102.2 eV, in addition to the band at 103.4 eV characteristic for Si atoms in Si gels (Figure 2a).<sup>[28]</sup> A detailed explanation of the spectra is presented elsewhere.<sup>[29]</sup>

The location of the MoO<sub>x</sub> particles in the MoO<sub>x</sub>/support composite, was determined by TEM-EDAX (transmission electron microscopy/energy-dispersive X-ray analysis) measurements. This method was employed to measure the chemical composition of selected primary particles observed in TEM images of composite samples. The TEM micrographs of pure Al-MCM-41 and three MoO<sub>x</sub>/Al-MCM-41 composites obtained ultrasonically at different Mo/support ratios are depicted in Figure 3. The composites consist of friable aggregates of Al-MCM-41 crystals and almost spherical 50–200 nm particles of MoO<sub>x</sub> phase. At low Mo content (21 wt % MoO<sub>3</sub>, Figure 3b) no spherical MoO<sub>x</sub> particles were detected (on looking at 15 different 85 × 85 μm areas of the sample). Only one ≈200 nm spherical-particle agglomerate with >90 wt % MoO<sub>3</sub> content (Figure 3c) was found in the 45 % MoO<sub>3</sub> sample. At an MoO<sub>3</sub> content of 66 wt % many separate spherical 40–60 nm particles of pure MoO<sub>x</sub> phase (Figure 3d)

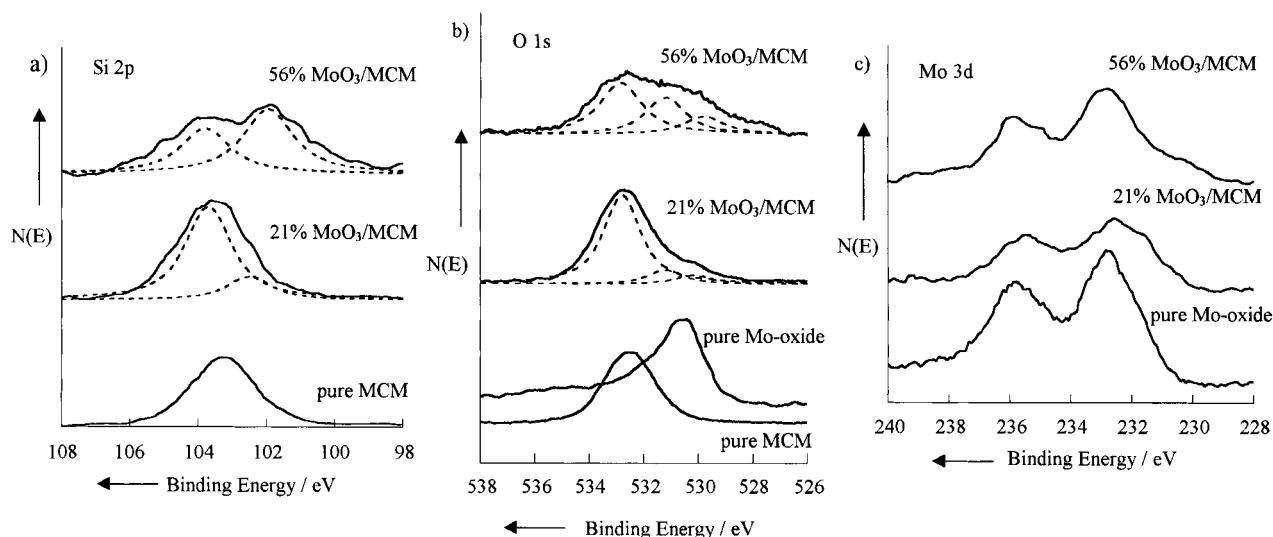


Figure 2. a) Si 2p, b) O 1s, and c) Mo 3d XPS spectra of sonochemically synthesized MoO<sub>x</sub>/Al-MCM-41 compared with the bare support and unreacted MoO<sub>x</sub>.

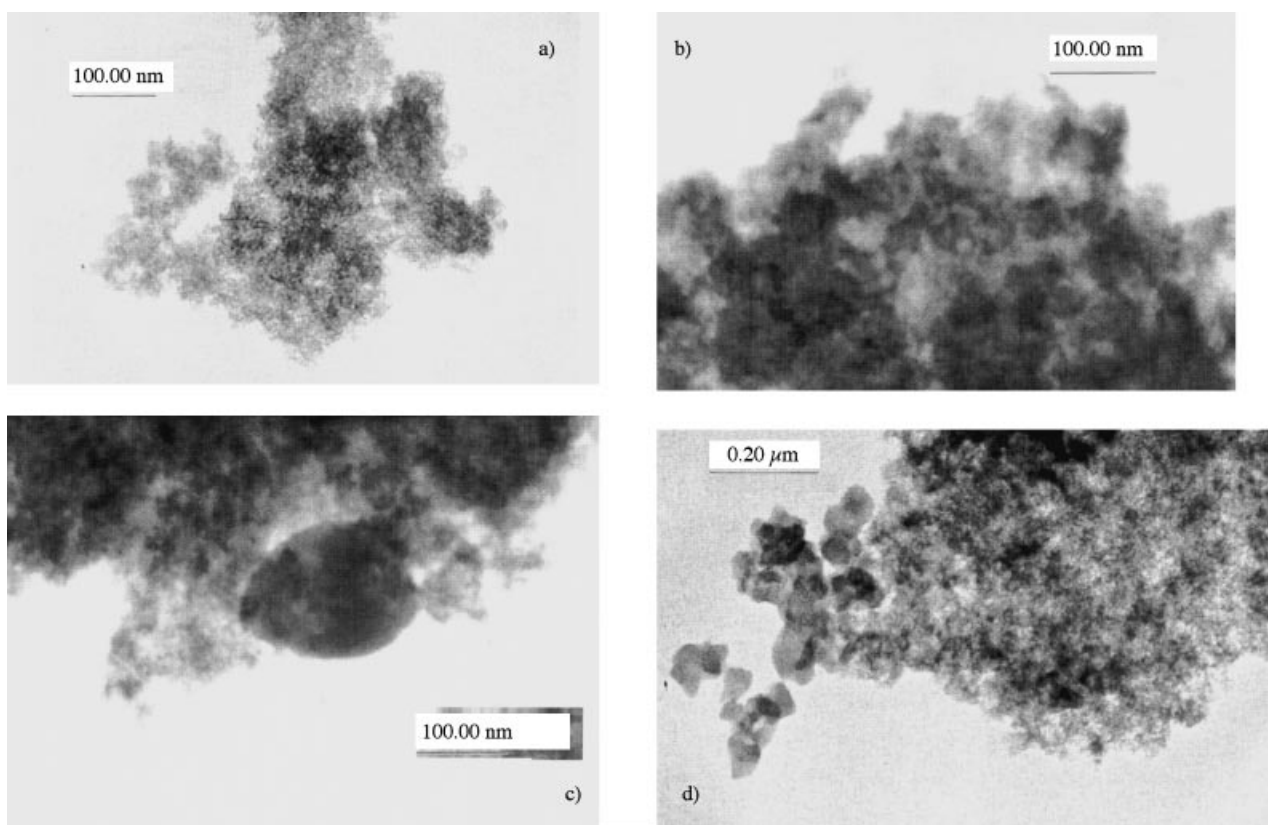


Figure 3. TEM micrographs of the Al-MCM-41 support and MoO<sub>3</sub>/Al-MCM-41 composite. a) Al-MCM-41; b) 21% MoO<sub>3</sub>/Al-MCM-41; c) 45% MoO<sub>3</sub>/Al-MCM-41; d) 66% MoO<sub>3</sub>/Al-MCM-41.

were observed. The data clearly demonstrates that the Mo oxide phase is located inside the support's pores and does not form separate particles up to an MoO<sub>3</sub> content of about 40–45 wt % upon ultrasonic deposition. High-resolution TEM (HRTEM) pictures reveal that the MoO<sub>3</sub> deposition does not cause degradation of Al-MCM-41 hexagonal pore structure.<sup>[29]</sup> In fact the HRTEM images clearly show the hexagonal nanotubes that form the pore structure of the support with walls thickness of ≈ 1.5 nm. It also shows that deposition

of MoO<sub>x</sub> increased the wall thickness to ≈ 2.3 nm. This is a result of formation of closed-packed monolayer of MoO<sub>x</sub> phase on the surface of Al-MCM-41 pores due to the ultrasonically controlled formation of surface Mo–silicate species.

Additional information about the location and state of MoO<sub>x</sub> phase in MoO<sub>x</sub>/Al-MCM-41 composites was obtained from the XRD patterns of thermally treated samples. As shown by Dhas and Gedanken,<sup>[26, 27]</sup> the Mo-blue oxide,

precipitated from a solution of  $\text{Mo}(\text{CO})_6$  in decalin under ultrasonication, is XRD amorphous and can be fully crystallized into a crystalline  $\text{MoO}_3$  phase by heating in air at  $300^\circ\text{C}$  for 48 hours. The  $\text{MoO}_x/\text{Al-MCM-41}$  composites with different Mo-loading, prepared by ultrasonically controlled HDP (homogeneous deposition–precipitation), were treated in these conditions after drying. The integral intensity of the  $\text{MoO}_3$  (020) reflection ( $2\theta = 12.8^\circ$ ), with respect to the calibration data, was used for estimating the content of the  $\text{MoO}_3$  phases in thermally treated samples. The XRD of the 21 and 45 wt %  $\text{MoO}_3$  samples reveals only a very small crystalline fraction ( $<5\%$ ) of  $\text{MoO}_x$ . Most of the  $\text{MoO}_x$  is located inside the pores in form of a close-packed monolayer, with chemical bonds between the  $\text{MoO}_x$  and the support. These bonds prevent its crystallization into  $\text{MoO}_3$  bulk particles. At a higher Mo-loading of 66 wt % significant amounts of  $\text{MoO}_x$  phase crystallizes into  $\text{MoO}_3$  particles with domain diameters of 35 nm. Such particles are not located in Al-MCM-41 pores of 6–9 nm, but outside, in agreement with TEM data. It means that crystalline  $\text{MoO}_3$  could be thermally created only from the  $\text{MoO}_x$  phase precipitated outside the Al-MCM-41 mesopores. It confirms the chemical interaction of  $\text{MoO}_x$  phase with support surface in ultrasonically deposited composites and its location inside the support pores up to  $\text{MoO}_3$  loading 40–45 wt %.<sup>[29]</sup>

Considering the surface area of Al-MCM-41 used in this work and an Mo surface concentration of 5 Mo atoms  $\text{nm}^{-2}$ , the geometrical closed packed monolayer capacity corresponds to 50 wt %  $\text{MoO}_3$ , which is in the good agreement with our measurements.

The remaining question is what is the role of the ultrasound radiation in the insertion of the nanoparticles into the mesopores. It is clear that the bubble can not collapse inside the mesopores because the size that the bubble reaches before its collapse is estimated to be about 100 microns.<sup>[8]</sup> Instead our explanation is based on microjets and shock waves that result when a bubble collapses near a solid surface.<sup>[30]</sup> Cavitation near liquid–solid interfaces is very different from cavitation in pure liquids.<sup>[31]</sup> Near a solid surface the collapse drives high-speed jets of liquid into the surface. Since most of the energy is transferred to the accelerating jet, the jet can reach velocities of hundreds of meters per second. In addition, shockwaves created by cavity collapse may also induce surface damage. In our case the small nanoparticles are pushed by these jets into the mesopores and, as a result of their reaction with the mesoporous support, are anchored to the inner surface of the mesoporous material.

### The Use of the Sonochemically Prepared Mesoporous Composites in Catalysis

Two catalytic reactions have been examined with sonochemically prepared composites. The first, the hydrodesulfurization (HDS) of dibenzothiophene (DBT) on  $\text{MoO}_x/\text{Al-MCM-41}$ , the second the oxidation of cyclohexane on  $\text{Fe}_2\text{O}_3/\text{TiO}_2$ . Only the latter results will be presented.

**The procedure for cyclohexane oxidation:** The oxidation of cyclohexane was performed in a thermostated glass reactor with cyclohexane (2 mL, 18.5 mmol), isobutyraldehyde (2.5 mL, 27.75 mmol) (molar ratio 1.5:1), a catalytic amount of acetic acid (0.06 mL, 1 mmol), and an amount of the catalyst equivalent to 0.015 mmol of iron oxide. The reaction mixture was stirred magnetically at  $70^\circ\text{C}$  and 1 atm of oxygen for 15–17 hours. The reaction products were analyzed by GC by using the starting alkane as an internal standard. Conversion was defined as a percentage of the starting alkane converted into the products. In Table 1 we present the conversion of cyclohexane into oxidation products detected by using three forms of the catalyst: 1) unsupported nanophased amorphous  $\text{Fe}_2\text{O}_3$ ; 2) amorphous  $\text{Fe}_2\text{O}_3$  deposited on  $\text{TiO}_2$  (Degussa P-25), which we have reported on previously,<sup>[32]</sup> and 3) amorphous  $\text{Fe}_2\text{O}_3$  deposited on mesoporous  $\text{TiO}_2$ . The last system showed the highest activity in the cyclohexane oxidation. The main products (selectivity almost 90%) were cyclohexanol and cyclohexanone in the ratio 1.5:1.

### Acknowledgements

A.G. thanks the German Ministry of Education and Research through the Deutsche-Israeli Program (DIP) for its financial support.

- [1] C. N. R. Rao, *J. Mater. Chem.* **1999**, 9, 1.
- [2] C. T. Kresge, M. E. Leonowicz, W. J. Roth, J. C. Vartuli, J. S. Beck, *Nature* **1992**, 359, 710.
- [3] J. S. Beck, J. C. Vartuli, W. J. Roth, M. E. Leonowicz, C. T. Kresge, K. D. Schmitt, C. T. W. Chu, D. H. Olson, E. W. Sheppard, S. B. McCullen, J. B. Higgins, J. L. Schlenker, *J. Am. Chem. Soc.* **1992**, 114, 10834.
- [4] A. Corma, *Chem. Rev.* **1997**, 97, 2373.
- [5] M. S. Whittingham, *Curr. Opin. Solid State Mater. Sci.* **1996**, 1, 227.
- [6] F. Schuth, *Curr. Opin. Colloid Interface Sci.* **1998**, 3, 174.
- [7] G. D. Stucky, A. Monnier, F. Schuth, Q. Huo, D. Margolese, D. Kumar, M. Krishnamurty, P. Petroff, A. Firouzi, M. Janicke, B. F. Chmelka, *Mol. Cryst. Liq. Cryst.* **1994**, 240, 187.
- [8] *Ultrasound: Its Chemical, Physical and Biological Effects* (Ed.: K. S. Suslick), VCH, Weinheim, **1988**.
- [9] K. S. Suslick, S.-B. Choe, A. A. Cichowals, M. W. Grinstaff, *Nature* **1991**, 353, 414.
- [10] Y. Wang, X. Tang, L. Yin, W. Huang, A. Gedanken *Adv. Mater.* **2000**, 12, 1137.
- [11] X. Tang, S. Liu, Y. Wang, W. Huang, Yu. Koltypin, A. Gedanken, *Chem. Commun.* **2000**, 2119.
- [12] Y. Q. Wang, L. X. Yin, O. Palchik, Y. Rosenfeld Hachohen, Yu. Koltypin, A. Gedanken, *Langmuir*, submitted.
- [13] Y. Wang, L. Yin, A. Gedanken, *Langmuir*, submitted.
- [14] a) R. Ryoo, J. M. Kim, C. H. Ko, C. H. Shin, *J. Phys. Chem. B* **1996**, 100, 17718; b) R. Ryoo, S. Jun, *J. Phys. Chem. B* **1997**, 101, 317.
- [15] M. Yada, H. Kitamura, M. Machida, T. Kijima, *Inorg. Chem.* **1998**, 37, 6470.
- [16] G. S. Attard, J. C. Glyde, C. G. Goltner, *Nature* **1995**, 378, 366.
- [17] Y. Huang, W. H. Sachtler, *Chem. Commun.* **1997**, 1181.
- [18] M. Yada, H. Kitamura, A. Ichinose, M. Machida, T. Kijima, *Angew. Chem.* **1999**, 111, 3716; *Angew. Chem. Int. Ed.* **1999**, 38, 3506.
- [19] R. A. Salkar, P. Jeevanandam, S. T. Aruna, Yu. Koltypin, O. Palchik, A. Gedanken, *J. Phys. Chem. B* **2000**, 104, 893.
- [20] E. Briot, J. Y. Piquemal, M. Vennat, J. M. Brageault, G. A. Chottard, J. M. Manoli, *J. Mater. Chem.* **2000**, 10, 953.
- [21] a) Z. H. Luan, L. Kevan, *J. Phys. Chem. B* **1997**, 101, 2020; b) G. Grubert, J. Rathousky, G. Schulz-Ekloff, M. Wark, A. Zukal, *Microporous Mesoporous Mater.* **1998**, 22, 225.

- [22] J. R. Agger, M. W. Anderson, M. E. Pemble, O. Terasaki, Y. Nozue, *J. Phys. Chem. B* **1998**, *102*, 3345.
- [23] M. Haruta, B. S. Uphade, S. Tsubota, A. Miyamoto, *Res. Chem. Intermed.* **1998**, *24*, 329.
- [24] Z. W. Fu, Q. Lu, W. Zhang, D. Y. Zhao, Q. Z. Qin, *Acta Chim. Sin.* **2000**, *58*, 1226.
- [25] X. Cao, R. Prozorov, Yu. Koltypin, G. Kataby, A. Gedanken, *J. Mater. Res.* **1997**, *12*, 402.
- [26] N. A. Dhas, A. Gedanken, *J. Phys. Chem.* **1997**, *101*, 9495.
- [27] N. A. Dhas, A. Gedanken, *Chem. Mater.* **1997**, *9*, 3144.
- [28] D. Briggs, M. P. Sean, *Practical Surface Analysis, Vol. 1*, 2nd ed., Wiley, New York, **1990**.
- [29] Ultrasonically controlled deposition–precipitation. Co–Mo HDS catalysts deposited on wide-pore MCM material: M. V. Landau, L. Vradman, M. Herskowitz, Y. Koltypin, A. Gedanken, *J. Catal.* **2001**, in press.
- [30] K. S. Suslick, G. J. Price, *Annu. Rev. Mater. Sci.* **1999**, *29*, 295.
- [31] T. G. Leighton, *The Acoustic Bubble*, Academic Press, London, **1994**.
- [32] N. Perkas, Y. Koltypin, O. Palchik, A. Gedanken, S. Chandrasekaran, *Appl. Catal. A.* **2001**, *209*, 125.
-